Micromechanical Deformation and Recovery Processes of Nylon-6/Rubber Thermoplastic Vulcanizates As Studied by Atomic Force Microscopy and Transmission Electron Microscopy

J. Oderkerk,[†] G. de Schaetzen,[‡] B. Goderis,[§] L. Hellemans,[‡] and G. Groeninckx*[,†]

Department of Chemistry, Laboratory of Macromolecular Structural Chemistry, Katholieke Universiteit Leuven (KULeuven), Celestijnenlaan 200F, B-3001 Heverlee, Belgium; Department of Chemistry, Laboratory of Physical Chemistry, Katholieke Universiteit Leuven (KULeuven), Celestijnenlaan 200D, B-3001 Heverlee, Belgium; and DSM Research, P.O. Box 18, 6160 MD Geleen, The Netherlands

Received July 30, 2001; Revised Manuscript Received May 7, 2002

ABSTRACT: Thermoplastic vulcanizates (TPVs), as prepared by dynamic vulcanization, are blends in which cross-linked rubber particles are finely dispersed in a thermoplastic matrix. The reported nylon-6/EPDM TPVs show significant strain recovery behavior, even though the matrix consists of semicrystalline nylon-6, which deforms plastically via shear yielding. Atomic force microscopy and transmission electron microscopy experiments revealed an inhomogeneous plastic deformation of the matrix phase. During straining, the plastic deformation is initiated in those zones where the nylon matrix between the rubber particles is the thinnest. Even at high strains, the thick ligaments of the nylon matrix remain almost undeformed and act as adhesion points holding the rubber particles together. When the external force is removed, the elastic force of the stretched, dispersed rubber phase pulls back the plastically deformed nylon parts by either buckling or bending. This is considered to be the key mechanism for the elastic behavior of the investigated TPVs.

1. Introduction

Thermoplastic vulcanizates (TPVs) are blends of a thermoplastic polymer and a cross-linked synthetic rubber. The rubber is dynamically cross-linked during melt-blending, resulting in a fine dispersion of a high amount of rubber in the thermoplastic matrix[1]. In the present paper the TPV consists of a nylon-6 matrix and a maleic anhydride modified ethylene−propylene−diene terpolymer (EPDM-*g*-MA) as dispersed phase. These engineering TPVs were prepared according to a procedure described earlier.[2] Such thermoplastic vulcanizates display excellent elastic properties although the matrix phase consists of a semicrystalline thermoplastic polymer, which is expected to deform plastically via shear yielding.[3,4] The rubber phase orientation is proportional to the applied strain upon uniaxial deformation, as revealed by rheooptical Fourier transform infrared spectroscopy experiments.[3] A relatively high value for the orientation function of the rubber phase is found whereas the value corresponding to the nylon phase is rather low. These results were accounted for by introducing a microstructural model that assumes a very inhomogeneous plastic deformation of the nylon matrix during straining and a good adhesion between the nylon matrix and the dispersed rubber phase. The present atomic force microscopy (AFM) results essentially confirm this deformation model, and in addition they provide a better understanding of the high elasticity of these blend materials. Atomic force microscopy measurements have only very recently successfully been used to investigate the morphology changes during deformation of polymers and polymer blends.[5−8]

In the present paper thin films of nylon-6/rubber TPVs with a dispersion of 50 and 60 wt % rubber are deformed stepwise using a ministretching device in order to study the micromechanical deformation processes. AFM images are collected after each deformation step. Transmission electron microscopy (TEM) was used to study the deformation of the bulk of tensile bars, with special emphasis on the possibility of rubber cavitation.

2. Experimental Section

2.1. Materials. A low/medium molecular weight nylon-6 was used ($M_w \approx 25\,000$ kg/mol, $\rho = 1.14$ g/mL, trade name Akulon K123) and was kindly supplied by DSM. For the rubber phase a high molecular weight maleic anhydride modified EPDM (EPDM-*g*-MA) was used, as obtained from Uniroyal (1 wt % MA, E/P ratio 50/50, $\rho = 0.88$ g/mL, trade name Royaltuf 465).

The components were melt-mixed and dynamically vulcanized in a DSM mini-extruder for 6 min at a screw speed of 80 rpm and a temperature of 260 °C. The peroxide (0.25 wt %), as cross-linking agent, was first dissolved in mineral oil (2 wt %) before being premixed with the rubber in a Haake 69 cm^3 batch mixer. Subsequently, the nylon/rubber TPVs were compounded in the mini-extruder. The extruded strands were pelletized into granulates. Finally, the nylon/rubber blends were injection molded into tensile bars (70 × 5 × 2 mm, DIN 53 457 type 2A1/2) on a mini-injection molding machine (designed by DSM Research) at a melt temperature of 260 °C and a mold temperature of 100 °C. All AFM, TEM, and tensile tests were performed at room temperature.

2.2. Sample Preparation for AFM. Thin films for the AFM measurements were prepared by cryogenically microtoming samples obtained from the bulk of the injection molded bars at −100 °C using a Leica Ultracut ULT microtome equipped with a FCS-E cryostat and a diamond knife. As such, films with a very smooth surface were obtained with the following dimensions: length 13 mm, width 2 mm, and thickness 20 μm. The AFM investigations are performed on nylon-6/rubber TPVs with 50 and 60 wt % rubber.

2.3. AFM Measurements. The mini-stretching device for the AFM measurements at stepwise increasing deformation

† Laboratory of Macromolecular Structural Chemistry, KULeuven.
‡ Laboratory of Physical Chemistry, KULeuven.
§ DSM Research.
* To whom correspondence should be addressed. E-mail: gabriel.groeninckx@chem.kuleuven.ac.be.

10.1021/ma0113475 CCC: $22.00
Published on Web 07/16/2002

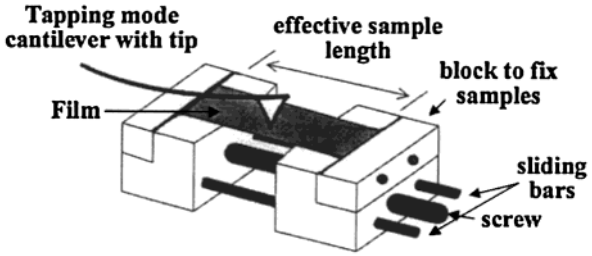

Figure 1. Mini-stretching device for AFM measurements.

has a maximum size of 17 mm × 10 mm and a height of 10 mm (see Figure 1). It was borrowed from Dr. S. Hild of the University of Ulm, Department of Experimental Physics, who designed it.[5] The sample, which must have a length of about 13 mm, can be mounted in the device as shown in Figure 1. The effective sample length measures 3 mm when both clamping jaws are close together. One jaw is fixed; the second one is mounted onto two sliding bars, which can be moved by turning a fine pitch thread screw. Emery paper is glued on these blocks to avoid slipping of the foils during stretching. The maximum elongation that can be reached is 7 mm.[5] The elongation can be tuned in steps of 0.1 mm by turning the screw. The distance between the two clamping jaws is measured using a sliding gauge and converted into a stretching ratio. To avoid vibrations of the film, an additional support was placed underneath while scanning. For the same reason a small stress was applied over the samples in the mini-stretching device right from the start. This small stretching, which is below 5%, accounts for the particles that are slightly elongated along the *y*-axis for samples that are nominally not stretched.

Tapping mode AFM height and phase images[9] were recorded simultaneously in air using a Dimension 3000 (Digital Instrument, Santa Barbara, CA) equipped with a J-scanner. The built-in optical microscope enables scanning in approximately the same area after each elongation step. Putting the probe at exactly the same spot was, however, impossible. Measurements on different sample positions were compared and revealed a fairly homogeneous morphology on 10 μm scale images. Moreover, in another experiment, a series of subsequent measurements were performed on the same spot of a stretched sample, revealing hardly any changes with time and hence the nominal absence of relaxation phenomena. Early, fast relaxation phenomena that are finished after, say, 5 min escape the experiment since that is a typical time to get started with an actual scan after the application of a given deformation.

During scanning the cantilever was excited at its resonance oscillation frequency, and the amplitude was kept constant at 90% of the free-air amplitude. Silicon tapping tips were used as provided by Nanosensors, Wetzlar, Germany (Pointprobe Non Contact/TappingTM-mode Sensors). The tip cantilevers are 225 μm long, resonate at 170 kHz, and have an average spring constant around 50 N m^{-1}. During scanning the amplitude of the cantilever oscillation varies due to the sample topography. To hold the oscillation amplitude and hence the average tapping force at a constant set-point level, the tip−sample separation is continuously readjusted. This adjustment results in a height image when plotted as a function of the probe's *x*/*y* coordinates on the sample. A so-called phase image is obtained when mapping the phase lag of the cantilever oscillation relative to that of the piezo drive. This phase lag depends on the topography as well as on local sample properties like adhesion, hydrophilicity, and (visco)elasticity. Therefore, experiments on heterogeneous materials such as immiscible polymer blends quite often yield images with a reasonable phase contrast between the separated components. The contrast in phase as well as in height images critically depends on the scanning parameters and may even invert.[10] Qualitatively, it can be stated that in the low-force, light tapping regime high-resolution images of surface features are produced whereas local differences in adhesion, hydrophilicity, and

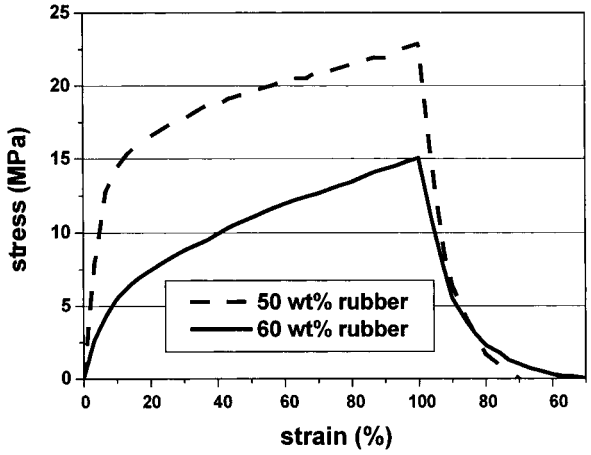

Figure 2. Tensile stress−strain (true stress) and recovery behavior of nylon-6/EPDM-*g*-MA TPVs based on 50 and 60 wt % rubber.

(visco)elasticity dominate the phase contrast in the hard tapping mode (oscillation amplitude much lower than the free-air amplitude).[11,12] Despite the fairly mild tapping conditions adopted here, the phase contrast is believed to be mainly generated by the huge difference in viscoelastic behavior between the nylon-6 and the rubber phase. Hard nylon-6 appears bright (high phase) and softer EPDM areas dark (low phase). The assignment of the component characteristic phase shifts (associated with the present scanning parameters) relies on proportionality between the (known) volume fractions of the components and the areas they represent in the images. Of course, particularly for the 50 wt % rubber sample it is relevant to mention that, in addition, the blend morphologies are actually known from earlier TEM work, facilitating a correct assignment.[3] Height images were collected simultaneously with the phase images. The contrast they show is inferior to that of the phase images, and as such they are not included in this paper.

2.4. Sample Preparation for TEM. Specimens for TEM micrographs were taken from the injection molded tensile bars, which were stretched to 50 and 100% strain at a constant rate of 20%/min. Thin slices were cut from the bulk of the tensile bars, parallel to the stretching direction. The sample temperature during microtoming was −100 °C, and the knife temperature was −55 °C. The samples were fixed and stained with an osmium tetroxide/formaldehyde solution before cutting. Some sections were additionally stained with ruthenium tetroxide vapor for 15 min to enhance the staining of the rubber phase. The sections were imaged with a Philips CM 10 transmission electron microscope using an accelerating voltage of 80 kV. Samples with 20, 50, and 60 wt % rubber were examined.

2.5. Tensile Recovery Tests. Reference tensile-recovery tests were performed on thin films similar to those used for AFM. Such samples were stretched using a mini-stretching device (FSK, load cell = 100 N) at a constant strain rate of 20%/min for 5 min up to a total strain of 100%. Subsequently, the strain direction was reversed until a zero force was attained. In fact, similar curves are discussed in ref 3. In this earlier work also the tensile-recovery behavior of the pure components was discussed. Nylon-6 has a modulus of 2690 MPa and a remaining strain of 90% upon recovery, whereas the modulus of the rubber component is 3 MPa and the remaining strain only 20%.

3. Results and Discussion

3.1. Tensile Stress−Strain and Recovery Behavior. Figure 2 illustrates the tensile stress−strain and recovery behavior of the nylon-6/EPDM-*g*-MA TPVs with 50 and 60 wt % dispersed rubber phase, respectively. Macroscopically, both blend compositions deform

homogeneously, i.e., without necking. The tensile stress−strain curves of the samples clearly differ, although the rubber is dispersed in the nylon matrix in *both* cases.[2,3] The *E*-modulus and the yield stress are lower and the yield point (yield point area) is broader for the 60 wt % rubber sample as compared to the 50 wt % rubber sample. Such non-composite-like, rubbery behavior such as that of the 60 wt % rubber sample shows up for TPVs with a high rubber content when the interparticle distance drops below a critical value and the particles tend to touch each other.[13] A region of nearly constant slope up to 100% strain follows the yield point region of both samples.

The recovery part displays a remaining strain of 70% for the 50 wt % rubber sample and only 50% for the 60 wt % rubber sample. The deformation behavior of both blends is somehow strange since it is expected to reflect mainly that of the nylon matrix phase, which displays a high modulus (2690 MPa) and a poor recovery (90% remaining strain)[3] due to plastic deformation by shear yielding.[4]

These results together with the morphological data presented below are taken into account at the proposal of a deformation and recovery mechanism.

3.2. Tensile Deformation Behavior of Nylon/Rubber TPVs As Revealed by AFM. Parts a and b of Figure 3 represent the AFM phase images of non-strained nylon-6/EPDM-*g*-MA TPVs with 50 and 60 wt % of rubber, respectively. A very fine dispersion of the (dark) EPDM phase in the (bright) nylon matrix can be seen. This is due to the reactive compatibilization and dynamic vulcanization, as described in detail in a previous paper.[2] A rubber particle size distribution between 0.2 and 0.8 μm was claimed earlier for both blend compositions on the basis of TEM evidence.[3] Larger sample areas are covered in the present AFM images, which in principle allows for a statistically more relevant estimation. Clearly, a number of larger rubber particles are present in the 60 wt % rubber sample. The nylon areas that interconnect the rubber particles are not evenly thick throughout the samples. This nylon phase thickness heterogeneity is most pronounced for the 60 wt % rubber sample (Figure 3b), which exhibits an important fraction of very thin nylon ligaments. Note that some rubber particles are slightly oriented along the *y*-axis in this sample because of the slight stress that had to be applied to this thin film to get stable images as mentioned in section 2.3.

Figure 4 visualizes the morphology upon deformation of the 60 wt % rubber TPV at stepwise increasing strain. The first image is taken at 25% strain, after which it is increased in steps of 25% up to 100% strain with the collection of an AFM image at each step (Figure 4a−d).

The phase image at 100% strain (Figure 4d) clearly points to a very inhomogeneous deformation distribution within the material; the aspect ratio (L/D) of some rubber particles equals 3 or more, whereas others, judging from their aspect ratio, apparently are not deformed at all ($L/D = 1$). Most (if not all) of the nondeformed rubber particles are rather small and surrounded by thicker nylon areas, which implies that the latter are less susceptible to deformation compared to their thinner counterparts. Here it is assumed that the nylon phase around a particular rubber particle is deformed as much as the rubber particle itself. The nylon phase probed by this AFM technique does not reveal any particular texture whether deformed or not,

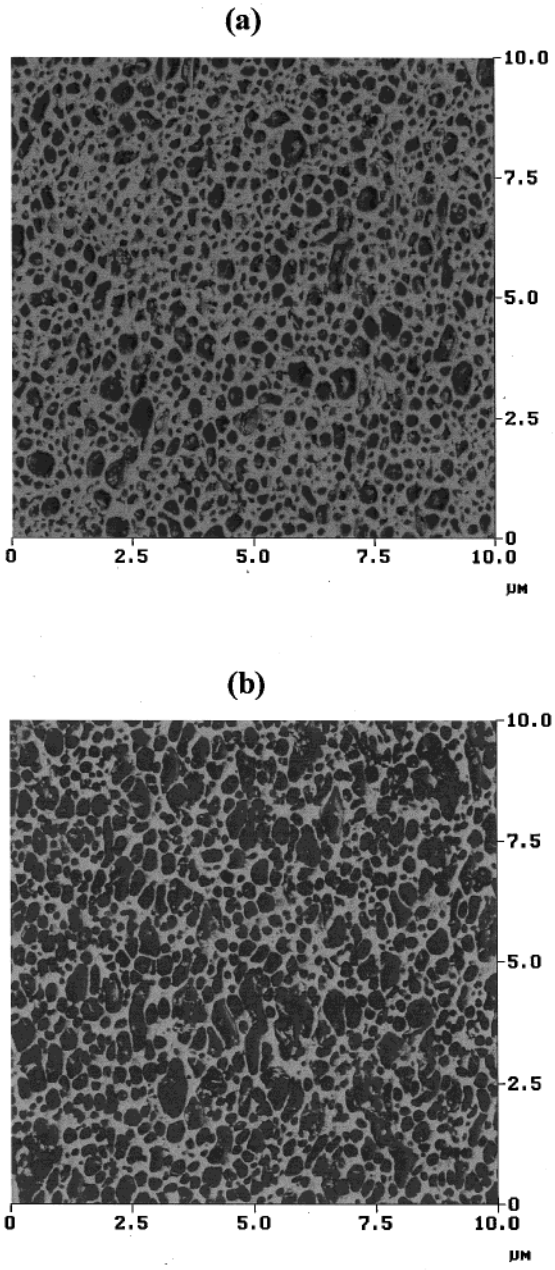

Figure 3. (a) AFM phase image of a nylon-6/EPDM-*g*-MA TPV with 50 wt % rubber. (b) AFM phase image of a nylon-6/EPDM-*g*-MA TPV with 60 wt % rubber.

impelling its deformation to be derived indirectly. The nylon-6 phase is below or close to T_g, which means that there is little difference in mechanical behavior between amorphous and crystalline nylon-6 and hence little or no contrast for phase imaging.

The preferential deformation of the thinner nylon parts can also be observed in Figure 5, which is an AFM phase image of the 50 wt % rubber TPV at 100% (overall) strain. This inhomogeneous deformation, however, is less pronounced compared to that of the 60 wt % rubber sample because a higher nylon content is accompanied by a narrower nylon phase thickness distribution (compare parts a and b of Figure 3).

An inhomogeneous deformation is compatible with previous IR strain investigations[3] and explains the stress−strain curves. Most likely, the force exerted on the sample is not equally transferred to all nylon parts because the sample is mechanically inhomogeneous. The

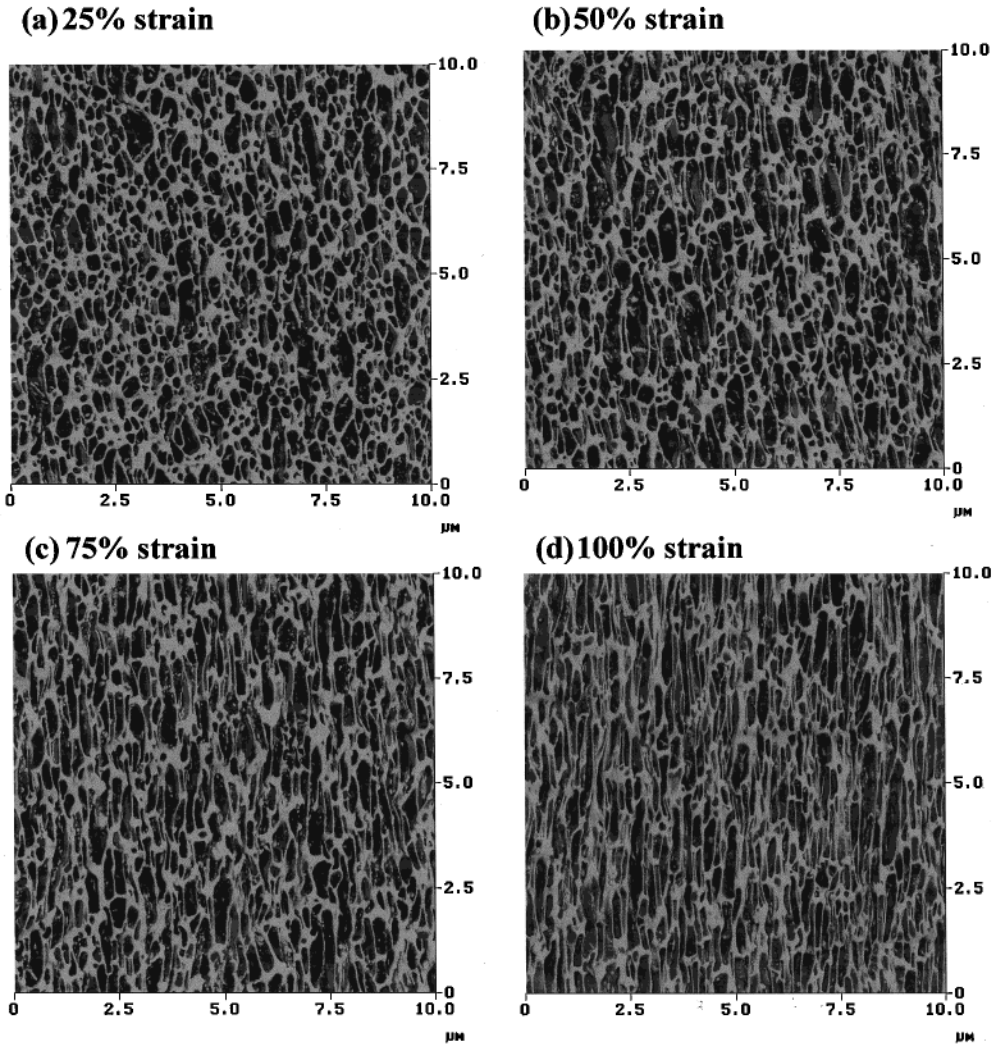

Figure 4. AFM phase images of a nylon-6/EPDM-*g*-MA TPV with 60 wt % rubber as a function of strain: (a) 25%, (b) 50%, (c) 75%, and (d) 100%; strain is applied in the vertical direction of these images.

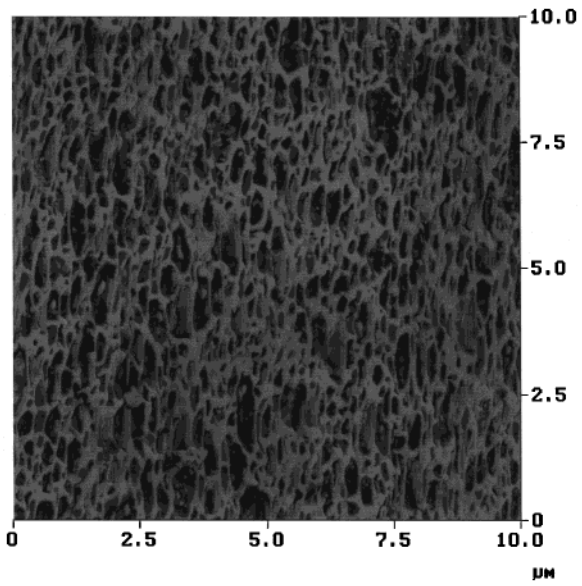

Figure 5. AFM phase image of a nylon-6/EPDM-*g*-MA TPV with 50 wt % rubber stretched until 100% strain; strain is applied in the vertical direction of this image.

local force on a particular nylon ligament may depend on the local two-phase morphology of the sample. However, if one assumes that an equal force is exerted on all nylon ligaments, then the stress on a particular ligament would only be inversely proportional to its thickness in a direction perpendicular to the direction of macroscopic strain. As a result, thin nylon regions deform *selectively* at a relatively low overall stress, and they deform plastically as soon as the local stress, which is the ratio of the force to the *local* cross-section area, exceeds the characteristic nylon yield stress. The next step upon further elongation is the local strain hardening of the yielded thin nylon parts. These stiffer parts no longer deform and transfer the stress onto nonyielded thicker nylon areas, which in turn may start to deform, yield, and strain harden. Consequently, nylon areas with increasing thickness are involved progressively at increasing overall strain. The very thick nylon regions may remain almost undeformed at any time, acting like rigid blocks holding the rubber particles together. This gradual stress-transfer mechanism is thought to hold for both the 50 and 60 wt % rubber sample and may account for the constant and equal slopes in the stress–strain curves beyond the respective yield stress regions. The initial slope, which is the *E*-modulus, as well as the macroscopic yield stress of a given TPV sample may, according to this view, very well be proportional to the thickness of the thinnest nylon ligaments present in the sample. The *E*-modulus of the 60 wt % rubber TPV–

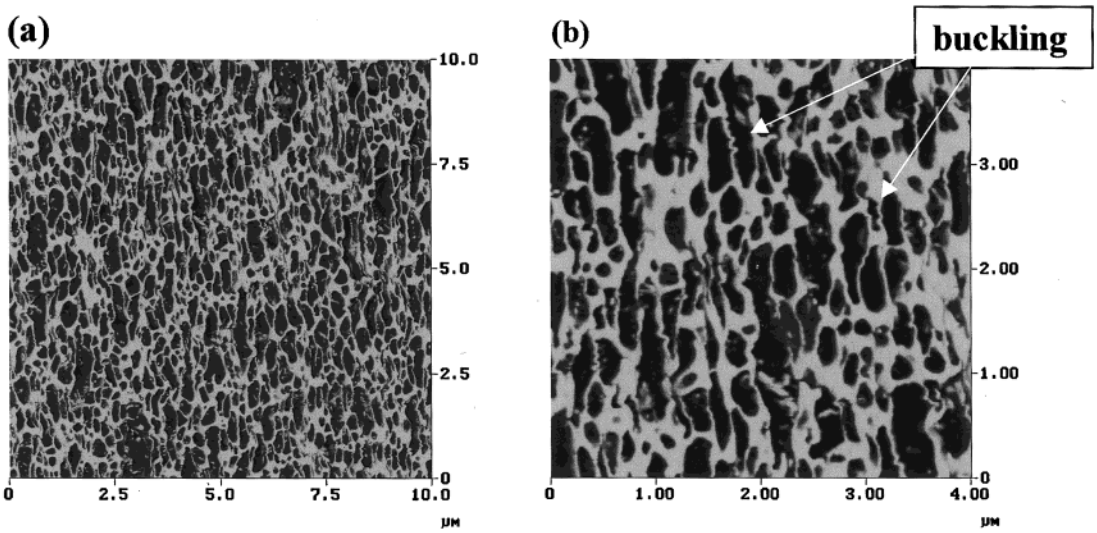

Figure 6. AFM phase images ((a) and (b): different magnifications) of a stress released nylon-6/EPDM-*g*-MA TPV film with 60 wt % rubber, after an applied strain of 100% (recovery 50%); strain was applied in the vertical direction of these images.

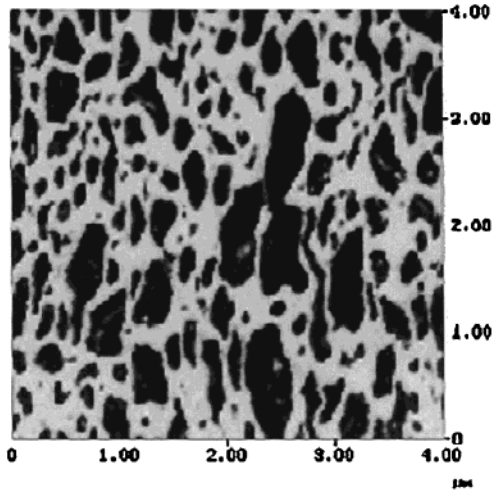

Figure 7. AFM phase image of a stress released nylon-6/EPDM-*g*-MA TPV film with 50 wt % rubber, after an applied strain of 100% (recovery 33%); strain was applied in the vertical direction of these images.

the sample with an important fraction of very thin nylon ligaments—is below that of the 50 wt % rubber TPV.

For sure, the nylon ligament thickness distribution is crucial in the understanding of the details of the macroscopic stress strain behavior. However, it goes beyond the scope of this article to elaborate these ideas into a mathematical model.

3.3. Tensile Recovery Behavior of Nylon/Rubber TPVs As Revealed by AFM. The nylon-6/EPDM-*g*-MA TPVs display good elasticity behavior,[2,3] despite the fact that the matrix consists of nylon-6, which normally deforms plastically during stretching. Apparently, the elastic restoring forces in the rubber particles are sufficiently high to engage the highly stretched and plastically deformed nylon parts in the action of recovery. It was anticipated that they bend or buckle during this process.[3] Such a morphology is revealed by AFM on stress released films, which were previously deformed to 100% strain. Figures 6 and 7 illustrate this observation for the 60 and 50 wt % rubber samples, respectively.

Buckling of the thin nylon fibrils is particularly clear in Figure 6b. The thicker ligaments, however, keep their original shape during the entire loading−unloading cycle or regain their original shape in the case of a limited amount of local deformation. Kikuchi et al.[14,15] and Kawabata et al.[16] suggested that these undeformed matrix regions hold the rubber particles together and that this continuous substructure of interconnected rubber particles accounts for the high degree of elastic recovery.

As can be seen from Figure 2, the recovery of the 50 wt % rubber sample is below that of the 60 wt % rubber sample. Figure 7 reveals that the degree of buckling of the nylon ligaments is indeed lower in the 50 wt % rubber sample. Apparently, the elastic restoring forces of the stretched rubber particles are too low to pull back the stretched thick nylon ligaments, which are thicker than the very thin ones present in the TPV sample with 60 wt % rubber.

3.4. Cavitation Behavior of the Rubber Phase during Deformation. Clearly, the elastic force of the rubber phase and the interfacial adhesion are very important for the strain recovery of TPVs. Consequently, recovery will be poorer if the rubber particles cavitate or debond upon deformation. The rubber particles dispersed in the matrix act as stress concentrators once a uniaxial tensile stress is applied to the tensile bar. This is due to differences in the Poisson's ratio and the intrinsic modulus of the matrix and the dispersed rubber phase.[17−21] Such a stress concentration leads to a local transition from an uniaxial to a triaxial (hydrostatic) stress state, possibly giving rise to void formation through cavitation inside the rubber particles or debonding at the particle−matrix interface. Dompas et al.[17,18] and Dijkstra et al.[19,20] found that cavitation already occurred before the actual yield point is reached for PVC/MBS and nylon-6/EPM-*g*-MA blends with low rubber contents (lower than 20 wt %). The influence of a higher rubber content on the cavitation behavior has not been reported in the literature yet.

Figure 8 presents TEM micrographs from the bulk of nylon-6/EPDM-*g*-MA tensile bars with 20 and 60 wt % rubber, respectively. The specimens were strained up to 100%, which is well beyond the yield point of these samples in a standard tensile test. Debonding does not occur in any of the samples because reactive compatibilization, as applied during melt-blending, renders the

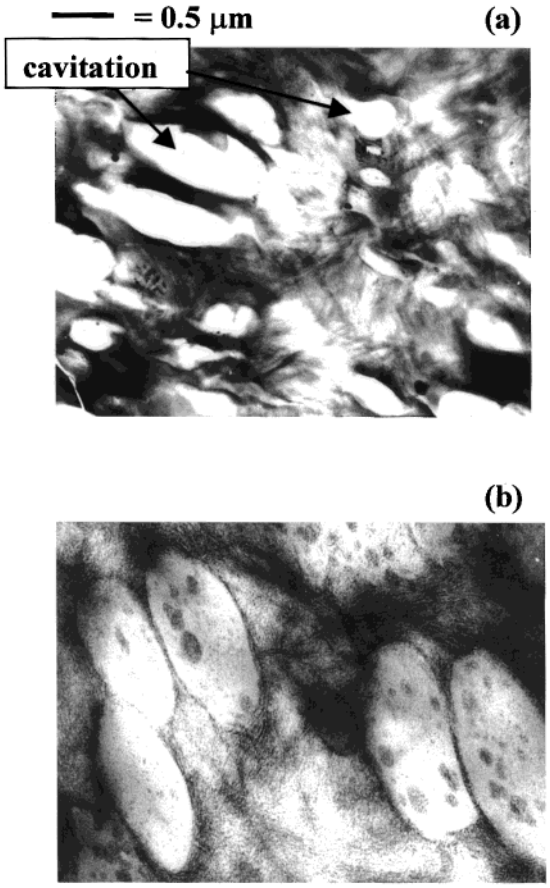

Figure 8. TEM micrographs after a strain test (100%) for (a) a blend with 20 wt % rubber and (b) a TPV with 60 wt % rubber (the arrows indicate cavitation in the rubber particles).

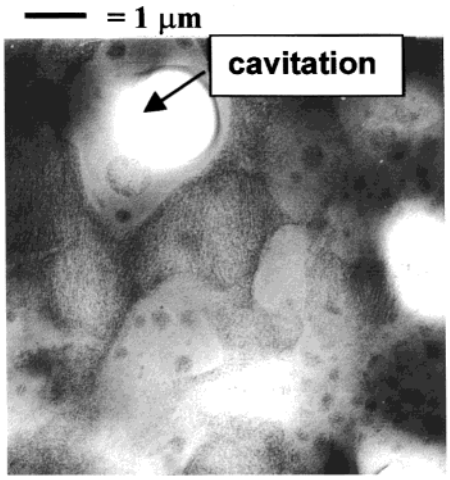

Figure 9. TEM micrograph of a nylon-6/EPDM-*g*-MA TPV with 50 wt % rubber after a strain test (100%) (the arrow indicates cavitation in the rubber particle).

interface between the rubber and the nylon phase very strong.[2] On the other hand, cavitation of the rubber particles is clearly observed for the 20 wt % rubber blend (Figure 8a), whereas the nylon/rubber TPV with 60 wt % rubber does not exhibit cavitation (Figure 8b). TEM micrographs were also taken from a TPV with 50 wt % rubber after applying a strain of 50% and 100%, which are both beyond the yield point of this particular sample. There is cavitation for an applied strain of 100% (Figure 9), but to a much lower extent as compared to the 20 wt % rubber blend. Note that in Figure 8b nylon inclusions can be observed in the rubber particles.

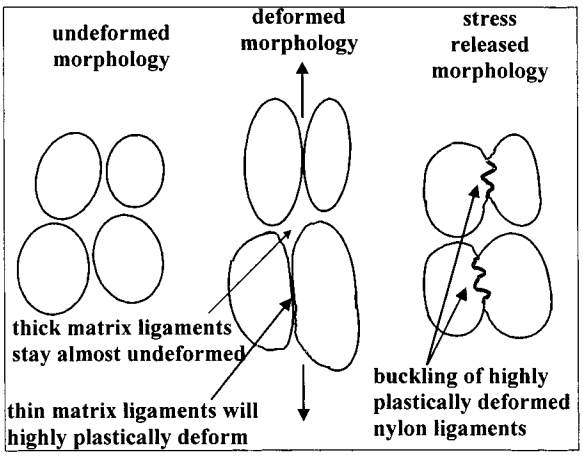

Figure 10. Sketch illustrating the deformation and recovery behavior of the nylon-6/EPDM-*g*-MA TPV systems.

For nylon-6/EPDM-*g*-MA TPVs with a high amount of rubber, the triaxial stress on the rubber particles is not high enough for inducing cavitation inside the rubber particles. The very thin nylon ligaments present in such TPVs readily yield by which stress is released and by which in turn a buildup of a hydrostatic stress in the rubber particles, sufficient for inducing cavitation, is avoided.

Finally, it should be mentioned that cavitation was not observed in any of the AFM images. Clearly, rubber particles that are at the surface of the sample experience another stress state compared to those of the bulk. The triaxial stress state, needed for cavitation, is not reached at the surface. Only a post mortem analysis of the bulk by means of TEM reveals the presence or the absence of cavitation correctly. AFM is superior in imaging steps during the deformation and readily revealed the deformation and recovery behavior of the nylon matrix. TEM and AFM in this particular case are truly complementary.

4. Conclusions

Morphology investigations using atomic force microscopy and transmission electron microscopy yielded detailed information on the deformation and recovery behavior of the rubber and the matrix phase in thermoplastic/rubber TPVs during uniaxial stretching and subsequent stress relaxation. The main features are illustrated in Figure 10.[3]

It appears that the inhomogeneous deformation of the nylon matrix is crucial to achieve the high elasticity of these nylon-6/rubber TPVs. During stretching, the matrix of nylon/rubber TPVs deforms inhomogeneously, the plastic deformation initially being concentrated in those areas where the nylon matrix is the thinnest. Thicker parts of the nylon matrix deform progressively at increasing overall strain. At each stage undeformed nylon ligaments act as adhesion points holding the rubber particles together. When the applied force is removed from the sample, the elastic forces of the stretched rubber particles pull back the highly plastically deformed thin nylon parts by either buckling or bending. Deformed thicker nylon parts are less susceptible to such recovery explaining why a 50 wt % rubber sample displays poorer recovery compared to a 60 wt % rubber sample. Besides the presence of thin matrix

ligaments, a good adhesion between the matrix and the rubber phase is a prerequisite for a good strain recovery, which in the present case is accomplished by reactive phase compatibilization. Strain recovery can be deteriorated by internal cavitation of the rubber particles. At a rubber content above 50 wt %, the investigated nylon-6/EPDM-*g*-MA TPVs display no cavitation.

Acknowledgment. The authors are indebted to DSM Research (Geleen, The Netherlands) for the financial support of this project as well as to the Fund for Scientific Research Flanders (FWO-Vlaanderen) and the Research Council of the KULeuven (GOA project 98/06) for equipment.

References and Notes

(1) Coran, A. Y. In *Thermoplastic Elastomers, A Comprehensive Review*; Legge, N. R., Holden, H. E., Schroeder, H. E., Eds.; Hansers Publishers: Munchen, 1987.
(2) Oderkerk, J.; Groeninckx, G. *Polymer* **2002**, *43*, 2219.
(3) Oderkerk, J.; Groeninckx, G.; Soliman, M. *Macromolecules* **2002**, *35*, 3946.
(4) Groeninckx, G.; Dompas, D. In *Structure and Properties of Multiphase Polymeric Materials*; Araki, T., Tran-Cong, Q., Shibayama, M., Eds.; Marcel Dekker: New York, 1998; Chapter 12.
(5) Hild, S.; Gutmannsbauer, W.; Lüthi, R.; Fuhrmann, J.; Güntherodt, H. J. *J. Polym. Sci., Part B: Polym. Phys.* **1996**, *34*, 1953.
(6) Drechsler, D.; Karbach, A.; Fuchs, H. *Surf. Interface Anal.* **1997**, *25*, 537.
(7) Coulon, G.; Castelein, G.; G'Sell, C. *Polymer* **1998**, *40*, 95.
(8) Oderkerk, J.; Groeninckx, G.; Soliman, M. Abstracts of the PPS-15 meeting, Hertogenbosch, The Netherlands, 1999.
(9) Zhong, Q.; Inniss, D.; Kjoller, K.; Elings, V. B. *Surf. Sci.* **1993**, *290*, 688.
(10) Knoll, A.; Magerle, R.; Krausch, G. *Macromolecules* **2001**, *34*, 4159.
(11) Magonov, S. *Polym. Mater. Sci. Eng.* **1998**, *78*, 106.
(12) Bar, G.; Thomann, Y.; Brandsch, R.; Cantow, H.-J. *Langmuir* **1997**, *13*, 3807.
(13) Oderkerk, J. Ph.D. Thesis, Katholieke Universiteit Leuven, 2000.
(14) Kikuchi, Y.; Fukui, T.; Okada, T.; Kikuchi, T. *Polym. Eng. Sci.* **1991**, *31*, 1029.
(15) Kikuchi, Y.; Fukui, T.; Okada, T.; Kikuchi, T. *J. Appl. Polym. Sci.: Appl. Polym. Symp.* **1992**, *50*, 261.
(16) Kawabata, S.; Kitawaki, S.; Arisawa, H.; Yamashita, Y.; Guo, X. *J. Appl. Polym. Sci.: Appl. Polym. Symp.* **1992**, *50*, 245.
(17) Dompas, D.; Groeninckx, G. *Polymer* **1994**, *34*, 4743.
(18) Dompas, D.; Groeninckx, G.; Isogawa, M.; Hasegawa, T.; Kadokura, M. *Polymer* **1994**, *35*, 4750.
(19) Dijkstra, K.; Van der Wal, A.; Gaymans, R. J. *Polymer* **1994**, *29*, 3489.
(20) Dijkstra, K.; ter Laak, J.; Gaymans, R. J. *Polymer* **1994**, *35*, 315.
(21) Kim, G. M.; Michler, G. *Polymer* **1998**, *39*, 5703.

MA0113475